



NLR-TP-2001-273

Practical investigation of aircraft pressure cabin MSD and corrosion

R.J.H. Wanhill, T. Hattenberg, W. van der Hoeven
and M.F.J. Koolloos



NLR-TP-2001-273

Practical investigation of aircraft pressure cabin MSD and corrosion

R.J.H. Wanhill, T. Hattenberg, W. van der Hoeven
and M.F.J. Koolloos

This report is based on a paper held at the 5th Joint NASA/FAA/DoD Conference on Aging Aircraft, HYATT-Orlando, Florida, September 2001.

The contents of this report may be cited on condition that full credit is given to NLR and the authors.

Division:	Structures and Materials
Issued:	15 June 2001
Classification of title:	Unclassified



Contents

SUMMARY	3
INTRODUCTION	3
FATIGUE	3
MSD Fatigue Initiation	3
Secondary Fatigue Initiation: B727-100	4
Early MSD Fatigue Crack Growth Rates	4
Environmental Effects: Early Fatigue Crack Growth	4
CORROSION	4
ASSOCIATIONS BETWEEN FATIGUE AND CORROSION	5
MSD FATIGUE MODELLING AND SIMULATION TESTING	5
General Remarks	5
Eijkhout's Model of Early MSD Fatigue Behaviour	5
MSD Fatigue Simulation Testing	6
LAP SPLICE FATIGUE ANALYSIS	6
CONCLUSIONS	7
ACKNOWLEDGEMENTS	7
REFERENCES	7



PRACTICAL INVESTIGATION OF AIRCRAFT PRESSURE CABIN MSD AND CORROSION

R.J.H. Wanhill, T. Hattenberg, W. van der Hoeven and M.F.J. Koolloos
National Aerospace Laboratory NLR, P.O. Box 153, 8300 AD Emmeloord, The Netherlands

SUMMARY

Longitudinal lap splices from several types of transport aircraft pressure cabins were investigated for Multiple Site Damage (MSD) fatigue and corrosion. The lap splices came from five service aircraft, three Fokker F28s, a British Aerospace BAC 1-11 and a Boeing B727-100; and a full-scale test on a Fokker F100. The results are compared with NASA data for a Boeing B747-400 full-scale test and information from the Boeing B737-200 Aloha Airlines accident.

INTRODUCTION

Aircraft are susceptible to fatigue and corrosion damage. There may be interactions between fatigue and corrosion, especially in ageing aircraft. Of particular concern are the longitudinal lap splices of transport aircraft pressure cabins. Lap splices from several aircraft types were investigated by the NLR for Multiple Site Damage (MSD) fatigue and corrosion, see table 1, which also includes lap splices from other investigations.

Table 1 Service or test histories of the pressure cabin longitudinal lap splices

Aircraft type	Flights	Simulated flights	Problems	Investigators
F28-4000 (1)	43,870	126,250 @ 110 % design load	MSD	} [1]
(2)	43,323		MSD	
F100			MSD	
BAC 1-11	75,158		MSD	
B727-100	53,424		corrosion (internal)	
F28-1000	34,470		corrosion (external)	
B747-400		60,000 @ 100 % design load	MSD	NASA [2]
B737-200	89,680		MSD + corrosion	NTSB [3]

The lap splices listed in table 1 came from a variety of positions in the pressure cabins [1], and their configurations differed widely, as shown in figure 1. The single common feature, which is very important, is the skin material, 2024-T3 Alclad aluminium alloy sheet.

This paper reviews and compares the results of all three investigations with respect to (1) MSD fatigue cracking, (2) corrosion and any associations between fatigue and corrosion, and (3) modelling, simulation testing and analysis of lap splice fatigue.

FATIGUE

MSD Fatigue Initiation

Figure 2 shows the characteristic MSD fatigue crack locations and shapes. The F28-4000 dimpled lap splices and B737-200 “knife-edged” lap splices are uncustomary. Bearing this in mind, the most representative fatigue initiation sites were at faying surfaces near or at rivet hole corners. This means the faying surface condition (cladding, anodising, priming, interfay sealant, adhesive bonding) and rivet hole corner quality are very important. Also, fretting must play a role, if not always in crack initiation, then probably soon after and during early crack growth [4].



Another very important point, with reference to service aircraft, is no evidence that corrosion was directly involved in crack initiation [1, 3], i.e. corrosion pitting is not responsible for initiating MSD fatigue cracks in lap splices using 2024-T3 Alclad skins.

Secondary Fatigue Initiation: B727-100

The B727-100 lap splice had experienced severe internal corrosion (see the next main section of this review). There were small, secondary fatigue cracks, which usually initiated from intergranular corrosion cracking that had already spread away from the rivet holes. However, twelve fatigue cracks were found at six rivet holes, out of a total of eighty-one examined. None of these cracks initiated from corrosion pitting. Ten of them occurred inside the rivet holes in the inner sheet. This behaviour is unlike that of the most representative MSD fatigue cracks, see above. The secondary fatigue cracks most probably initiated owing to a combination of corrosion pillowing stresses [5] and the cyclic stresses from cabin pressurization and depressurization.

Early MSD Fatigue Crack Growth Rates

Figure 3 summarises the data, which were obtained fractographically *from different sources*: F28-4000, Wanhill (NLR); F100, Eijkhout [6] and Vermeulen (NLR); BAC 1-11, Hattenberg (NLR); B747-400, Piascik and Willard [2]; B737-200, Anon (Boeing) [3]. The data show the following important features:

- (1) All crack growth rates were above 10^{-8} m/cycle.
- (2) The transverse (through-thickness) crack growth rates were, on average, fairly constant and remarkably similar.
- (3) The longitudinal crack growth rates were also remarkably similar, considering the different aircraft types and lap splice configurations, figure 1.

Environmental Effects: Early Fatigue Crack Growth

Unlike fatigue initiation, there was evidence of local environmental effects on early MSD and secondary fatigue crack growth in service aircraft (F28-4000s, BAC-1-11, B727-100). The fatigue fracture surfaces showed varying amounts of post-cracking corrosion, but the local environments must have been fairly mild, as concluded independently [7], since otherwise the fracture surfaces would have been obliterated [8].

Of more interest are any effects during early MSD fatigue crack growth. Some fracture surfaces showed crystallographic-looking “beach marks” similar to topographical changes produced by very low cycle frequency tests in “dry” and “wet” air, e.g. figure 4. Thus the “beach marks” could indicate periodic changes in the local environment during early MSD fatigue crack growth (and also secondary fatigue crack growth [1]). Be that as it may, it is presently unknown whether the local environmental conditions have significant effects on early fatigue crack growth rates in the lap splices. More work needs to be done, and the NLR is pursuing and persevering with very low frequency tests in “dry” and “wet” air in the crack growth rate regime $10^{-8} - 10^{-7}$ m/cycle.

CORROSION

The B727-100 internally corroded lap splice was non-destructively inspected by the Institute for Aerospace Research (IAR), Ottawa, before shipping to the NLR for inspection and disassembly. Figure 5 summarises the results. Disassembly showed that only the severest cracks, nearly 95 % of which were due to intergranular corrosion and stress corrosion, were previously detected by inspections. Also, the DAIS imaging detected severe corrosion better than eddy current, since the BS640 position was found to be severely corroded after disassembly, and this had not been indicated by eddy current.



The F28-1000 externally corroded lap splice was disassembled and eddy current inspected for rivet hole cracks. Selected rivet holes, in areas of severe thinning, were opened up by tensile testing. No crack indications or actual cracks were observed. These results were unexpected since the lap splice sample came from a position known to be MSD-susceptible.

ASSOCIATIONS BETWEEN FATIGUE AND CORROSION

From the previous main sections of this review and the full results of the investigation [1] we draw the following two main conclusions with regard to fatigue and corrosion:

- (1) Fatigue initiation. There was no evidence of corrosion pitting initiating either MSD fatigue cracks in the F28-4000 and BAC 1-11 lap splices or secondary fatigue cracks in the B727-100 lap splice. Nor did severe external corrosion result in MSD fatigue cracks in the F28-1000 lap splice, even though this was in an MSD-susceptible position. A further point is that the Aloha Airlines accident investigation concluded that although corrosion contributed to the accident, it was not directly associated with MSD fatigue [3]. Thus from the practical evidence to date it would appear that pressure cabin longitudinal lap splices using 2024-T3 Alclad sheet have either an MSD fatigue problem or a corrosion problem, i.e. there is no primary association between corrosion and the initiation of MSD fatigue cracks.
- (2) Early fatigue crack growth. There was evidence of local environmental effects on early MSD and secondary fatigue crack growth in service aircraft. The local environmental conditions were fairly mild, as evidenced by the survival of the fracture surfaces. It is as yet unknown whether the early MSD fatigue crack growth rates are significantly influenced by the local environmental conditions.

MSD FATIGUE MODELLING AND SIMULATION TESTING

General Remarks

The fatigue behaviour of pressure cabin longitudinal lap splices is determined by complex stress distributions and the faying surface condition. The stress distributions are difficult – if not impossible – to quantify [11, 12], and realistic stress intensity factor solutions are unavailable for early MSD fatigue crack growth. Also, models of fatigue initiation at corrosion pits, e.g. [13], and inclusions in the aluminium alloy matrix [14] are inappropriate for 2024-T3 Alclad lap splices. We observed no evidence of corrosion pitting initiating fatigue cracks, and tests have shown several times that fatigue cracks initiate in the cladding, not the 2024-T3 matrix [15, 16].

Instead, at least for now, recourse must be made to solely empirical modelling that describes *the actual early MSD fatigue behaviour* seen in service aircraft and full-scale tests, e.g. Eijkhout's model [6], which is described next.

Eijkhout's Model of Early MSD Fatigue Behaviour

Figure 6 shows the model, which is based on (1) MSD fatigue cracks initiating at several sites near or at rivet hole corners, and (2) nearly constant transverse (through-thickness) crack growth rates and initially similar transverse and longitudinal crack growth rates, see figure 3.

There are three main assumptions: dc/dN is constant and equal to the initial crack growth rate in the longitudinal direction, Ae^{Ba_i} ; crack depth $c = 0$ at a_i , the "initiation length"; and quarter-circular crack fronts in the transition from transverse to longitudinal crack growth. These assumptions are convenient but not essential. The model can be used for non-constant dc/dN



and for crack initiation at rivet hole corners, i.e. $a_i = 0$ in figure 6. Also the model can be used for both non-countersunk and countersunk lap splice sheets.

Eijkhout’s model enables estimates of

- fatigue crack growth lives
- fatigue “initiation” lives, by subtracting crack growth lives from the total life: here the “initiation” life is taken to be the fatigue life beyond which there is a regular process of crack growth, specifically in the 2024-T3 aluminium alloy matrix
- fatigue “initiation” + crack growth lives at which cracks become through-thickness: this information is potentially useful for in-service inspection.

Also, the model can be made compatible with marker bands on fracture surfaces from full-scale tests, e.g. [2].

MSD Fatigue Simulation Testing

As figure 3 shows, early MSD fatigue crack growth rates are above 10^{-8} m/cycle. On the one hand, this means no difference between short and long fatigue crack growth behaviour [1], which would be expected to make simulation testing easier. But on the other hand, these crack growth rates are much higher than those observed from sub-scale specimen tests [17, 18]. This situation may change when improved stress analyses become available and are used for improving sub-scale specimen design and testing. However, it may turn out that reliance will still have to be made mainly on full-scale pressure cabin section or panel tests [19].

LAP SPLICE FATIGUE ANALYSIS

Currently there is a move to replace the traditional fatigue life S-N approach to establishing the inspection threshold. The intent is to establish the inspection threshold using fatigue crack growth analysis and tests, whereby it is assumed the structure contains initial flaws (Initial Quality Flaw Sizes, IQFS) and that a regular process of fatigue crack growth begins as soon as the aircraft enters service.

Figure 7 shows schematically the probable differences between actual early MSD fatigue crack growth and predictions that fit crack growth models to the IQFS values, using back-extrapolation because of the limit of macroscopic observations of crack growth during tests. The major incongruity is the modelling assumption that regular crack growth begins immediately, i.e. there is no fatigue “initiation” life. This assumption is incorrect. Table 2 gives estimates of the MSD fatigue “initiation” lives for the BAC 1-11 service aircraft and the F100 and B747-400 full-scale tests. The lives to first crack “initiation” are significant fractions of the total lives, bearing in mind that B747-type aircraft were designed for a service life of 20,000 flights. Thus it would seem inadvisable to discount or ignore the fatigue “initiation” life, however arguable its definition.

Table 2 Estimates of MSD fatigue “initiation” lives

Aircraft type	MSD rivet row	Flights or simulated flights	
		Flights to first crack “initiation”	Total flights
BAC 1-11	outer sheet } port	50,000	} 75,158
	upper row } starboard	56,000	
	inner sheet, lower row, port	47,000	
F100	outer sheet upper row	60,000	} 126,250
	inner sheet lower row	70,000	
B747-400	outer sheet upper row	5000 – 15,000	60,000



CONCLUSIONS

- (1) There is no primary association between MSD fatigue and corrosion for pressure cabin longitudinal lap splices using 2024-T3 Alclad sheet for the fuselage skins. MSD fatigue is not initiated by local corrosion (pitting), and severe corrosion did not result in MSD fatigue.
- (2) There was a strong tendency for MSD fatigue cracks to initiate at faying surfaces near or at rivet hole corners. This means the faying surface condition (cladding, anodising, priming, interfay sealant, adhesive bonding) and rivet hole corner quality are very important.
- (3) A distinction should be made between MSD fatigue initiation and crack growth. Estimated MSD fatigue “initiation” lives, based on the commencement of a regular crack growth process in the 2024-T3 aluminium alloy matrix, were significant fractions of the total lives. Thus it is inadvisable to discount or ignore the fatigue “initiation” life, however arguable its definition, and to model MSD fatigue solely as a regular crack growth process that begins as soon as an aircraft enters service.
- (4) Early MSD fatigue crack growth rates were remarkably similar and all above 10^{-8} m/cycle (or flight). These relatively high crack growth rates make questionable the usefulness and relevance of sub-scale specimen tests.
- (5) For the service aircraft the local environmental conditions during early MSD fatigue crack growth were fairly mild, not obliterating the fracture surfaces during years of service. It is as yet unknown whether these environmental conditions have significant effects on early MSD fatigue crack growth rates.
- (6) Conclusions (1) – (5) and the supporting data [1-3, 6] should be taken into account during further development of fatigue analysis methods for transport aircraft pressure cabin lap splices. In this respect we advocate further investigation of the usefulness of Eijkhout’s empirical *reality-based* model.
- (7) Following on from conclusion (1), although severe internal corrosion in a B727-100 lap splice and external corrosion of an F28-1000 lap splice did not lead to MSD fatigue, the B727-100 lap splice had small, secondary fatigue cracks. These initiated usually from intergranular cracks due to corrosion and stress corrosion, but sometimes occurred directly from rivet holes. The latter most probably initiated owing to a combination of sustained stresses due to corrosion pillowing and the cyclic pressurization stresses.
- (8) Disassembly of the B727-100 lap splice showed only the severest corrosion cracking had been previously detected by X-ray and eddy current non-destructive inspections. The enhanced optical non-destructive inspection technique DAIS was more sensitive to detecting the presence of severe corrosion than eddy current.

ACKNOWLEDGEMENTS

This investigation was sponsored partly by the Netherlands Department of Civil Aviation (RLD) and by the NLR’s in-house basic research programme.

REFERENCES

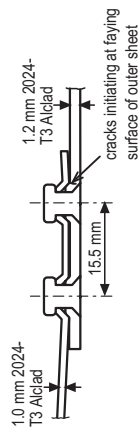
1. Wanhill, R.J.H., Hattenberg, T., Van der Hoeven, W., NLR CR-2001-256, National Aerospace Laboratory NLR, Amsterdam, June 2001.
2. Piasek, R.S., Willard, S.A., NASA TP-97-206257, National Aeronautics and Space Administration Langley Research Center, Hampton, Virginia, November 1997.
3. NTSB Report No. NTSB/AAR-89/03, National Transportation Safety Board, Washington, D.C., June 1989.



4. Rooke, D.P., AGARD Conference Proceedings No. 328, Advisory Group for Aerospace Research and Development, pp. 8-1 – 8-6 (1983): Neuilly-sur-Seine.
5. Bellinger, N.C., Komorowski, J.P., AIAA Journal, Vol. 35, pp. 317-320 (1997).
6. Eijkhout, M.T., Fokker Report RT2160, Fokker Aircraft Ltd., Amsterdam, November 1994.
7. Campuzano-Contreras, A.L., Arrowood, R.M., Murr, L.E., Little, D., Roberson, D., Niou, C.-S., Microstructural Science, Vol. 25, pp. 139-145 (1997).
8. Wanhill, R.J.H., Schra, L., Quantitative Methods in Fractography, ASTM STP 1085, American Society for Testing and Materials, pp. 144-165, Philadelphia (1990).
9. Wanhill, R.J.H., NLR TP 94177 L, National Aerospace Laboratory NLR, Amsterdam, June 1995.
10. Mussert, K.M., M. Sc. Thesis, Delft University of Technology, Delft, December 1995.
11. Eastaugh, G.F., Simpson, D.L., Straznicky, P.V., Wakeman, R.B., AGARD Conference Proceedings 568, Advisory Group for Aerospace Research and Development, pp. 2-1 – 2-19 (1995): Neuilly-sur-Seine.
12. Müller, R.P.G., An Experimental and Analytical Investigation on the Fatigue Behaviour of Fuselage Riveted Lap Joints, Delft University Press, pp. 17-39 (1995): Delft.
13. Cawley, N.R., Harlow, D.G., Wei, R.P., FAA-NASA Symposium on the Continued Airworthiness of Aircraft Structures, Report No. DOT/FAA/AR-97/2, Federal Aviation Administration, Part II, pp. 531-542, Washington, D.C., 1997.
14. Laz, P.J., Craig, B.A., Rohrbaugh, S.M., Hillberry, B.M., Fatigue '99, Engineering Materials Advisory Services Ltd., Vol. 2, pp. 833-838 (1999): Cradley Heath.
15. Forsyth, P.J.E., Problems with Fatigue in Aircraft, Eighth ICAF Symposium, Swiss Federal Aircraft Establishment (F+W), pp. 2.5/1 – 2.5/23 (1975): Emmen.
16. Schijve, J., Jacobs, F.A., Tromp, P.J., NLR TR 76065 U, National Aerospace Laboratory NLR, Amsterdam, July 1976.
17. Vlieger, H., Ottens, H.H., NLR CR 97139 L, National Aerospace Laboratory NLR, Amsterdam, April 1997.
18. Schra, L., Ottens, H.H., Vlieger, H., NLR CR 95279 C, National Aerospace Laboratory NLR, Amsterdam, June 1995.
19. Vercammen, R.W.A., Ottens, H.H., NLR TP 98148, National Aerospace Laboratory NLR, Amsterdam, March 1998.

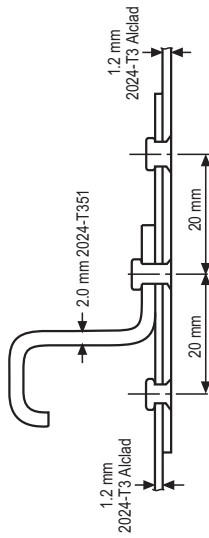
F28-Mk 1000/4000

- rivet pitch 16.6 mm
- rivet diameter 4 mm
- sheets dimpled instead of countersunk
- sheets chromic acid anodised and primed



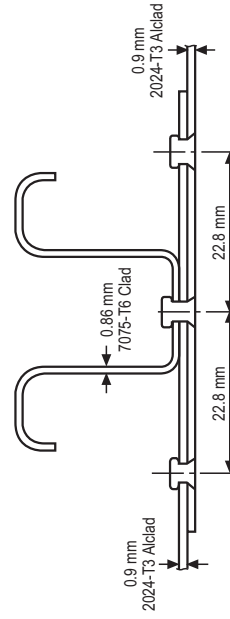
F100

- rivet pitch 20 mm
- rivet diameter 3.2 mm
- sheets chromic acid anodised, primed and cold bonded



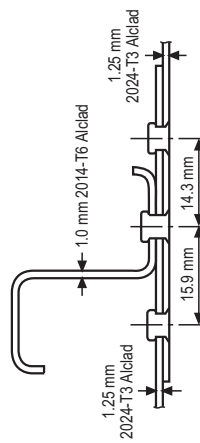
B737-200

- rivet pitch 25 mm
- rivet diameter 3.97 mm
- sheets cold bonded
- knife edges at outer sheet faying surface



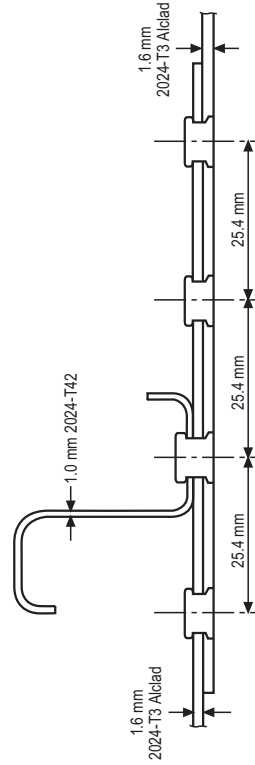
BAC 1-11

- stiffener rivet pitch 12.7 mm
- sheet rivet pitch 25.4 mm
- rivet diameter 3.2 mm
- sheets chromic acid anodised and primed
- interlay sealant



B747-400

- stiffener rivet pitch 20 mm
- sheet rivet pitch 30 mm
- rivet diameter 4.8 mm
- interlay sealant



B 727-100

- rivet pitch 28-30 mm
- rivet diameter 4.9-5.1 mm
- sheets and stiffener primed
- interlay sealant

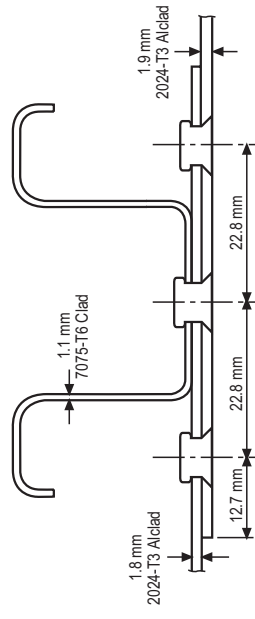


Fig. 1 Configurations of the lap splices. MSD fatigue: F28 Mk4000, F100, BAC 1-11, B747-400, B737-200. Corrosion: F28 Mk 1000, B727-100

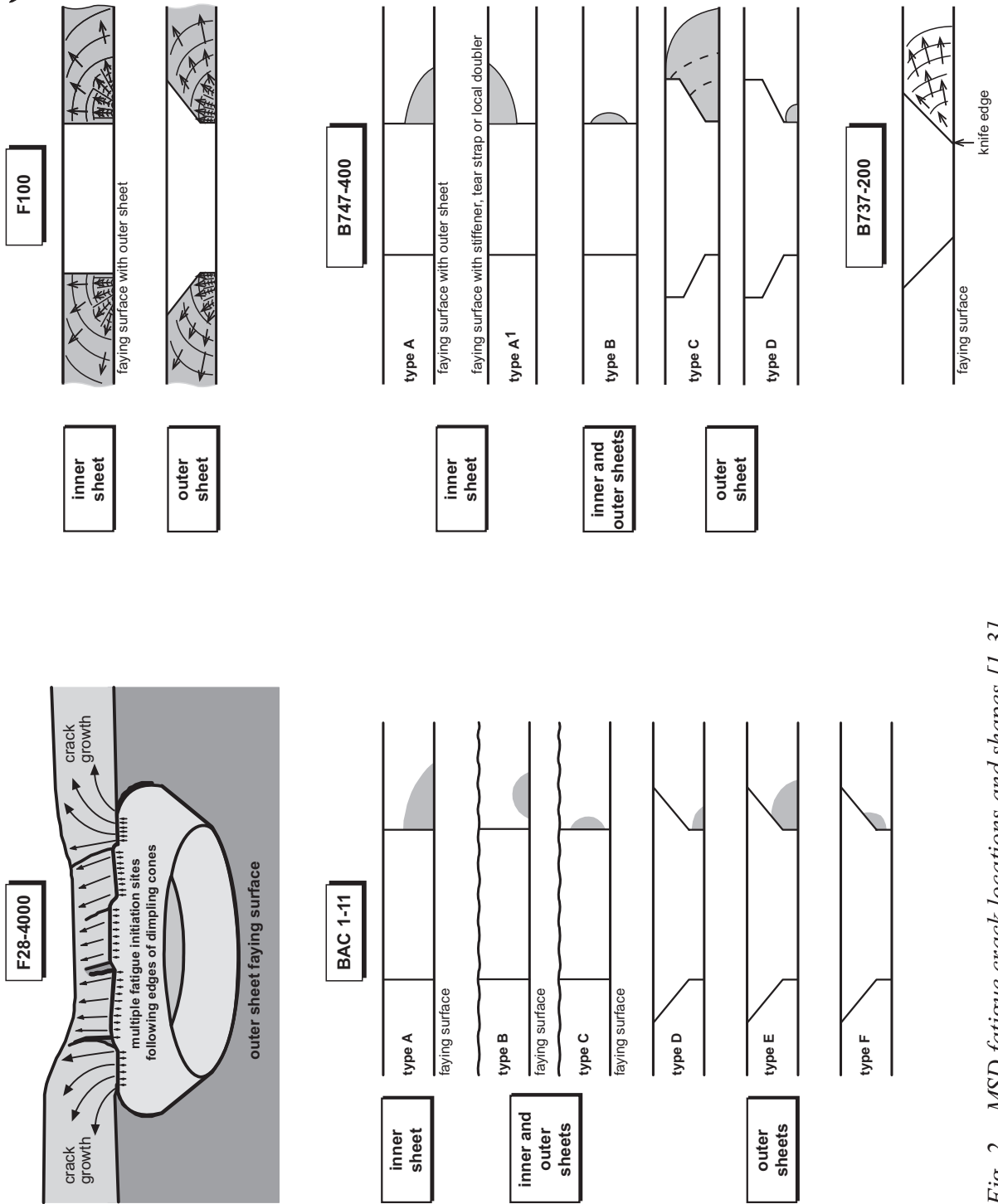


Fig. 2 MSD fatigue crack locations and shapes [1-3]

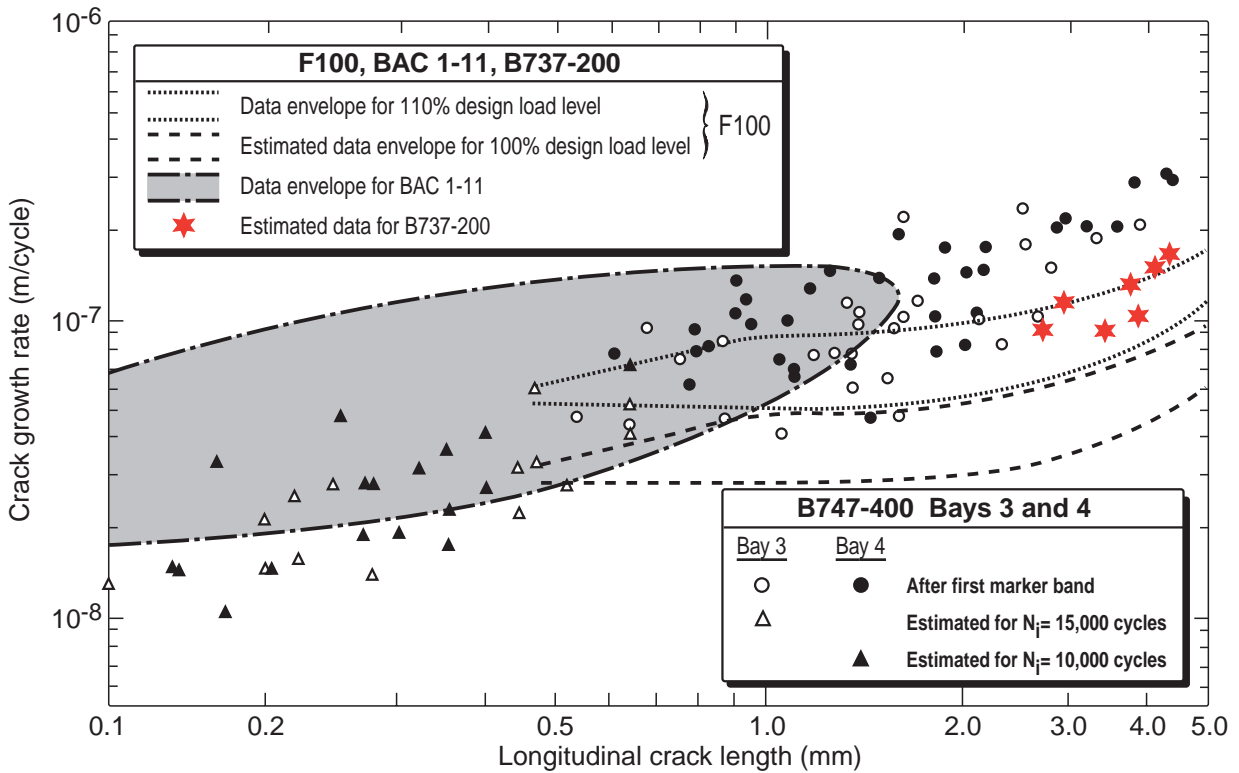
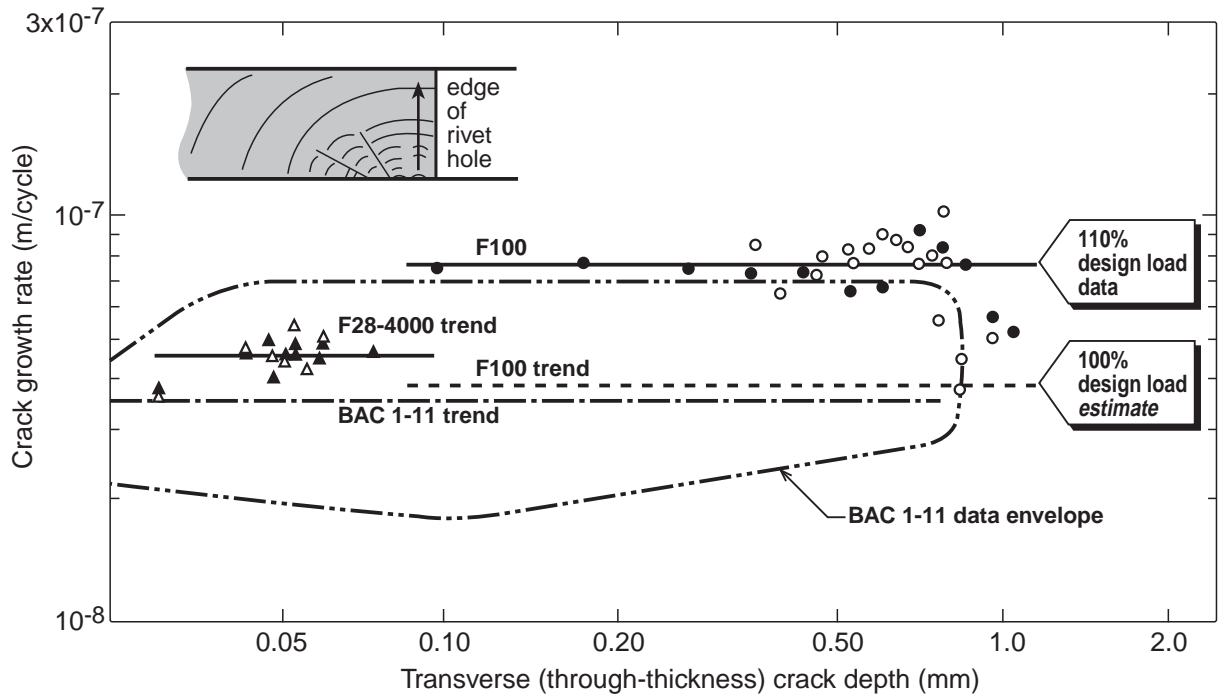
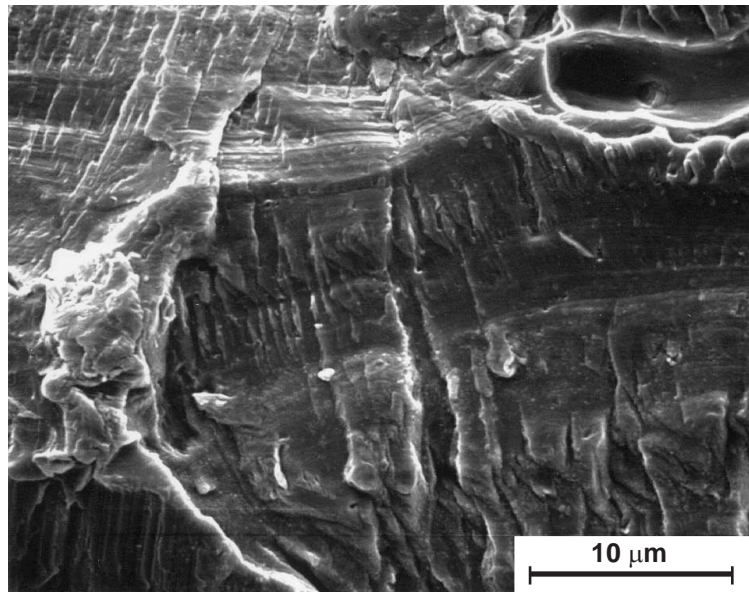


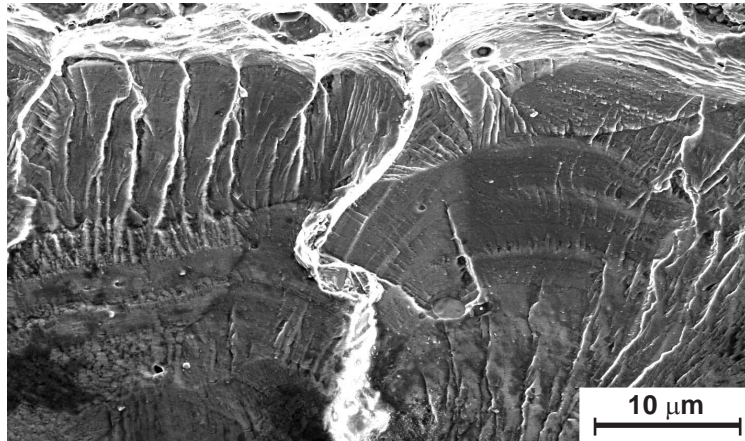
Fig. 3 Summary of transverse (through-thickness) and longitudinal early MSD fatigue crack growth rates [1, 2]. The F100 estimates were derived from the factor $(100/110)^{7.1}$, where 7.1 is the “Paris Law” exponent in the same crack growth rate regime [9]



F28-4000 (2)
Outer sheet



BAC 1-11
Outer sheet
starboard



2024-T3 sheet
0.003 Hz, R = 0.05
 $\Delta K \sim 8.5 \text{ MPa}\sqrt{\text{m}}$

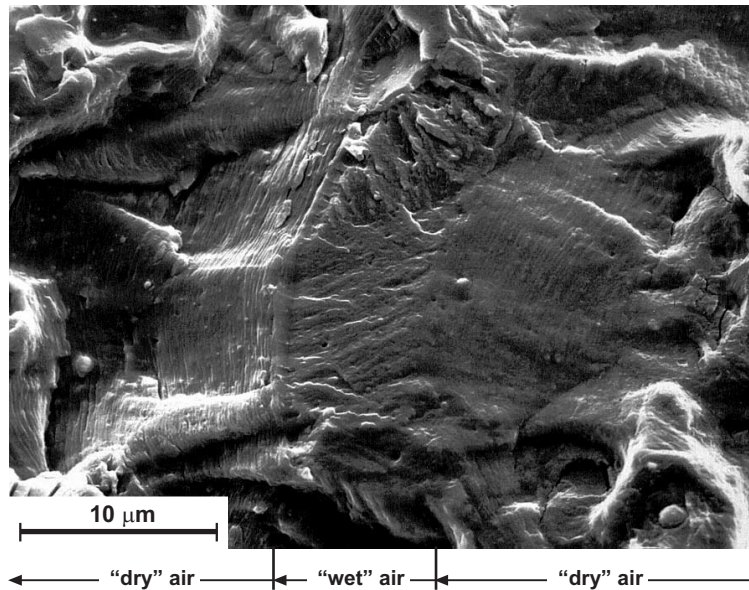
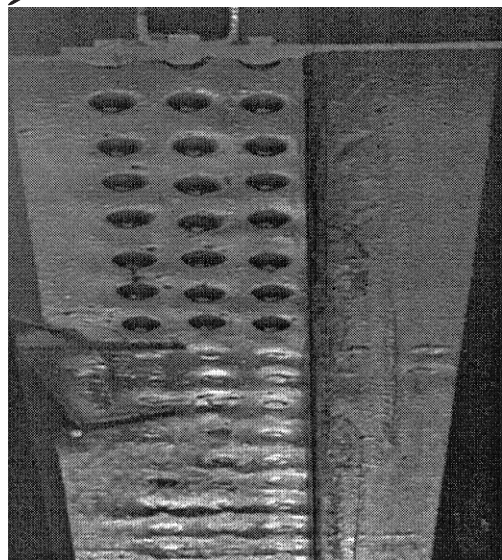
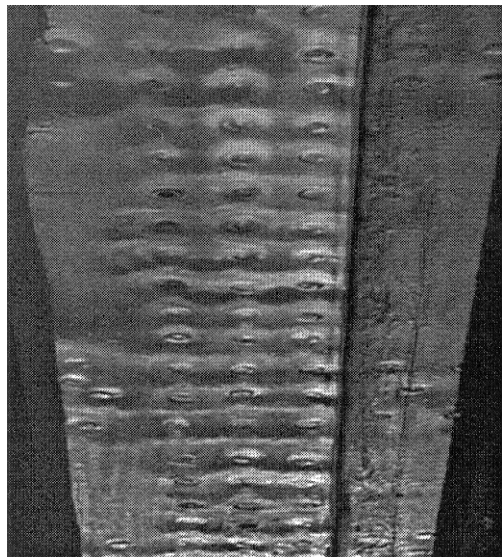


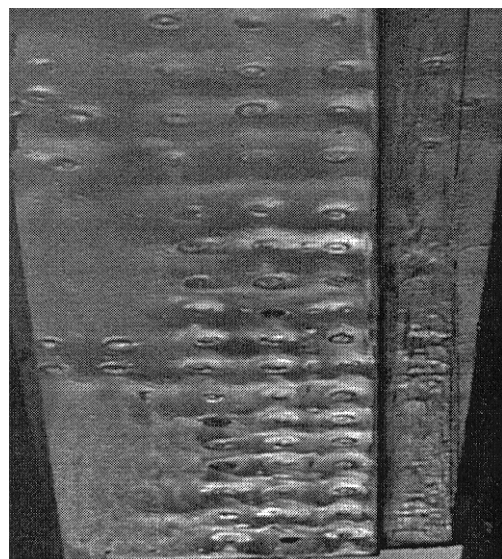
Fig. 4 Examples of “beach marks” for early MSD fatigue crack growth in service aircraft and similar topographical changes produced by very low cycle frequency tests in “dry” and “wet” air in the same crack growth rate regime [10]



BS600



BS620



BS640

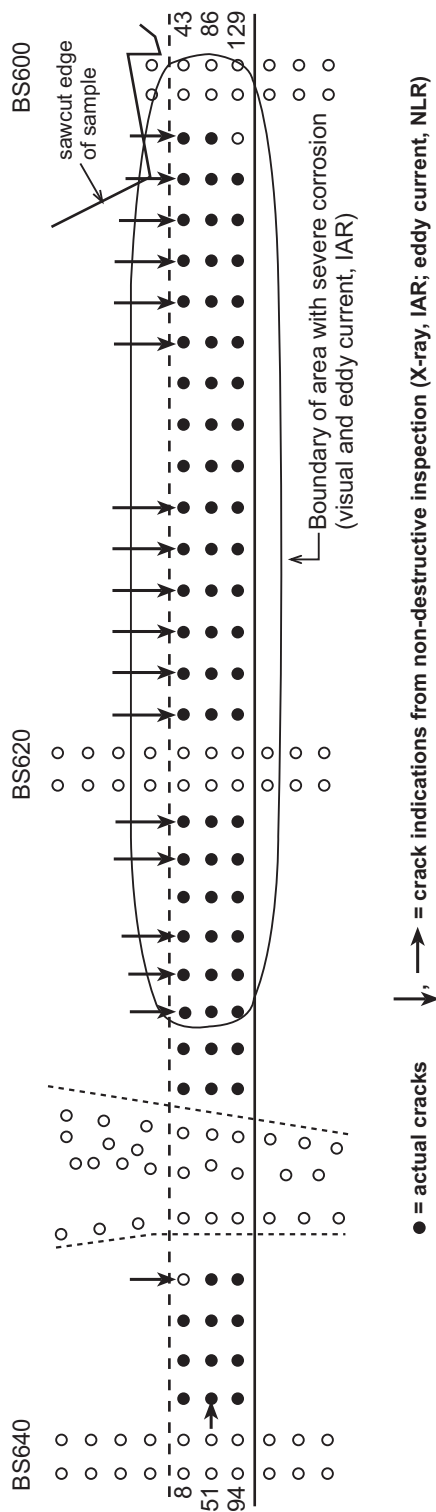
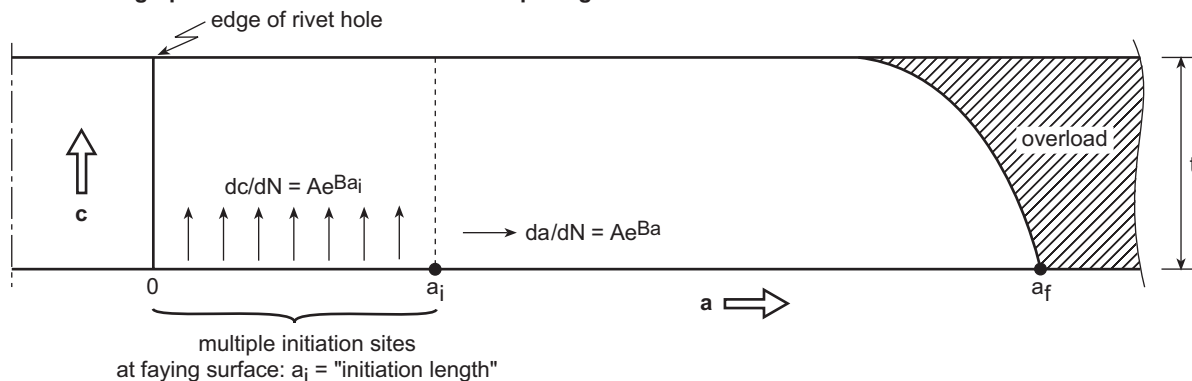


Fig. 5 DAIS imaging of corrosion-induced pilloving of the B727-100 lap splice (IAR) and schematic comparison of cracks found by non-destructive inspection (IAR, NLR) and lap splice disassembly (NLR): DAIS = D Sight Aircraft Inspection System, an enhanced optical method



- From fractographic observations and striation spacings:



- a_i, a_f and N_f are known. Calculate N_i from: $N_f - N_i = \frac{1}{AB} (e^{-Ba_i} - e^{-Ba_f})$
- Calculate intermediate values of a for given values of n : $a_{int} = -\frac{1}{B} \ln [e^{-Ba_i} - AB(N_{int} - N_i)]$
- For each a_{int} calculate c_{int} from: $c_{int} = (N_{int} - N_i) Ae^{Ba_i}$
- Construct crack fronts as follows:

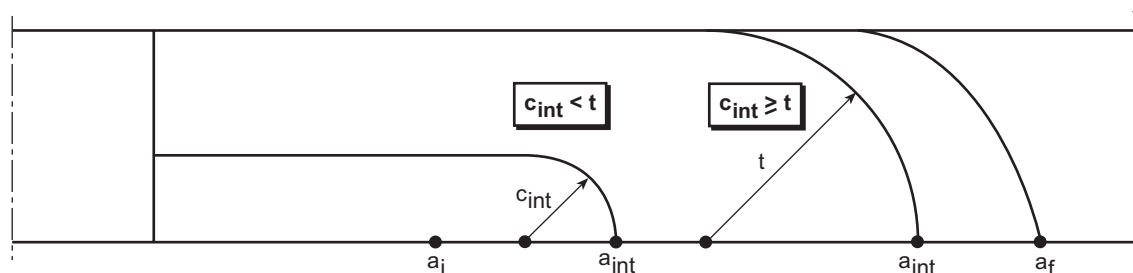


Fig. 6 Eijkhout's empirical model illustrated for a non-countersunk sheet and multiple fatigue initiation sites

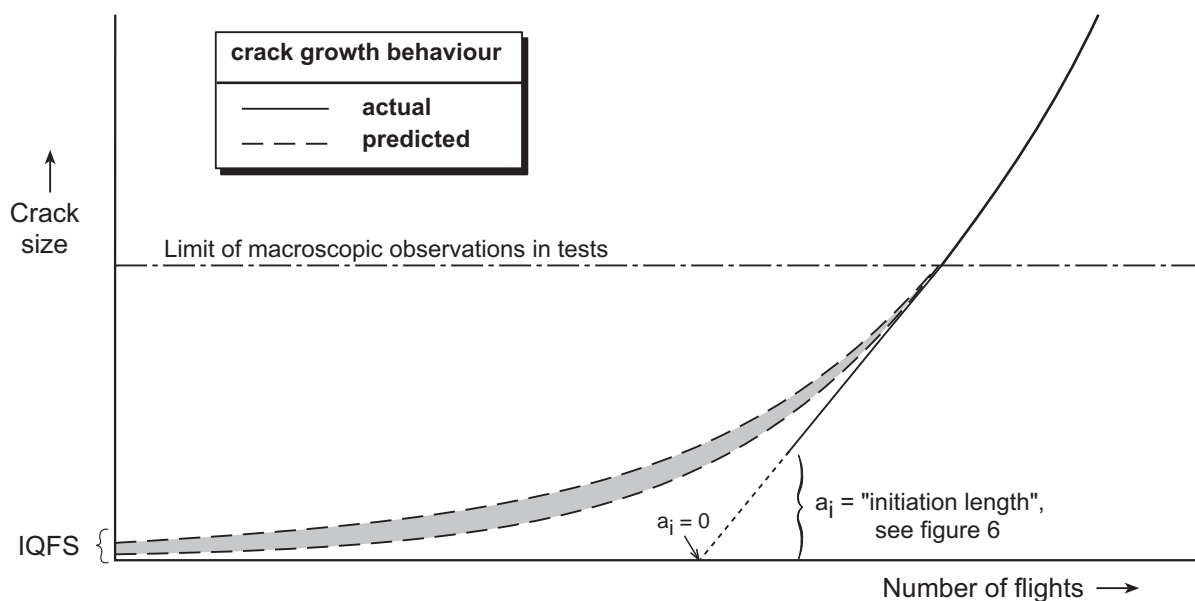


Fig. 7 Schematic of differences between actual and predicted early crack growth behaviour in transport aircraft fuselage longitudinal lap splices: the predictions are fitted to the macroscopic observations and the IQFS values are obtained from actual manufacturing flaws or by back-extrapolation using a macroscopic (long) crack growth model